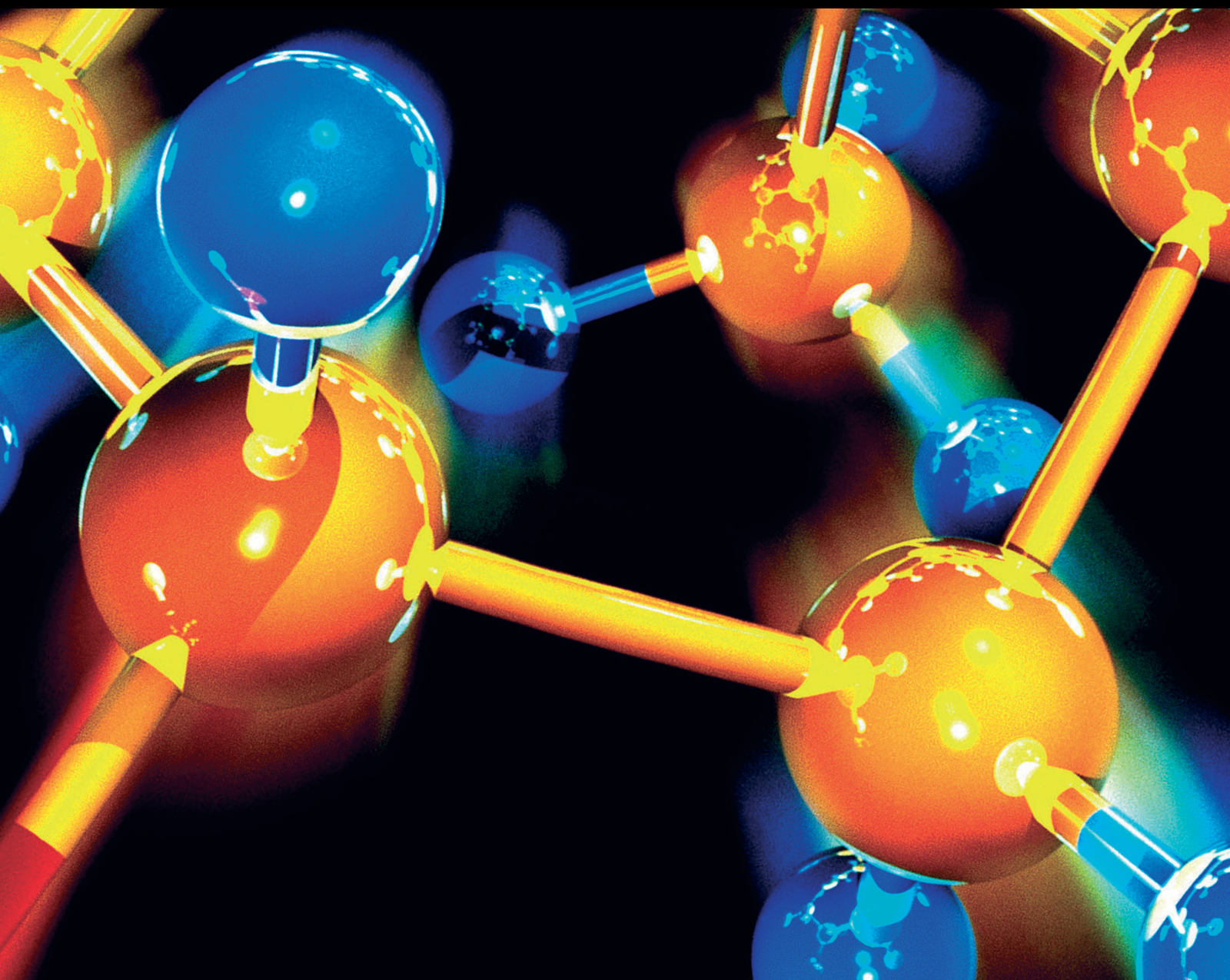


# Unconventional Reservoir Enhanced Oil & Gas Recovery from perspective of Chemistry

Lead Guest Editor: Wen-Dong Wang

Guest Editors: Harpreet Singh and Dongying Wang





---

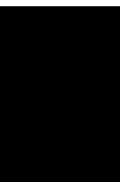
**Unconventional Reservoir Enhanced Oil & Gas  
Recovery from perspective of Chemistry**



**Unconventional Reservoir Enhanced  
Oil & Gas Recovery from perspective of  
Chemistry**

Lead Guest Editor: Wen-Dong Wang

Guest Editors: Harpreet Singh and Dongying Wang



---

Copyright © 2021 Hindawi Limited. All rights reserved.

This is a special issue published in "Journal of Chemistry." All articles are open access articles distributed under the Creative Commons Attribution License, which permits unrestricted use, distribution, and reproduction in any medium, provided the original work is properly cited.

# Chief Editor

Kaustubha Mohanty, India

## Associate Editors

Mohammad Al-Ghouthi, Qatar


Tingyue Gu , USA


Teodorico C. Ramalho , Brazil

Artur M. S. Silva , Portugal


## Academic Editors

Jinwei Duan, China

Luqman C. Abdullah , Malaysia

Dr Abhilash , India

Amitava Adhikary, USA

Amitava Adhikary , USA

Mozhgan Afshari, Iran

Daryoush Afzali , Iran

Mahmood Ahmed, Pakistan


Islam Al-Akraa , Egypt


Juan D. Alché , Spain

Gomaa A. M. Ali , Egypt

Mohd Sajid Ali , Saudi Arabia

Shafaqat Ali , Pakistan


Patricia E. Allegretti , Argentina

Marco Anni , Italy

Alessandro Arcovito, Italy

Hassan Arida , Saudi Arabia


Umair Ashraf, Pakistan


Narcis Avarvari , France

Davut Avci , Turkey


Chandra Azad , USA

Mohamed Azaroual, France

Rasha Azzam , Egypt


Hassan Azzazy , Egypt

Renal Backov, France

Suresh Kannan Balasingam , Republic of Korea

Sukanta Bar , USA

Florent Barbault , France

Maurizio Barbieri , Italy

James Barker , United Kingdom

Salvatore Barreca , Italy

Jorge Barros-Velázquez , Spain

THANGAGIRI Baskaran , India

Haci Baykara, Ecuador

Michele Benedetti, Italy

Laurent Billon, France

Marek Biziuk, Poland

Jean-Luc Blin , France

Tomislav Bolanca , Croatia

Ankur Bordoloi , India

Cato Brede , Norway


Leonid Breydo , USA


Wybren J. Buma , The Netherlands

J. O. Caceres , Spain

Patrizia Calaminici , Mexico


Claudio Cameselle , Spain


Joaquin Campos , Spain

Dapeng Cao , China

Domenica Capasso , Italy

Stefano Caporali , Italy

Zenilda Cardeal , Brazil


Angela Cardinali , Italy

Stefano Carli , Italy

Maria F. Carvalho , Portugal


Susana Casal , Portugal


David E. Chavez, USA

Riccardo Chelli , Italy

Zhongfang Chen , Puerto Rico

Vladislav Chrastny , Czech Republic

Roberto Comparelli , Italy

Filomena Conforti , Italy

Luca Conti , Italy


Christophe Coquelet, France

Filomena Corbo , Italy

Jose Corchado , Spain

Maria N. D.S. Cordeiro , Portugal

Claudia Crestini, Italy

Gerald Culioli , France

Nguyen Duc Cuong , Vietnam

Stefano D'Errico , Italy


Matthias D'hooghe , Belgium


Samuel B. Dampare, Ghana

Umashankar Das, Canada

Victor David, Romania

Annalisa De Girolamo, Italy


Antonio De Lucas-Consuegra , Spain

Marccone A. L. De Oliveira , Brazil

Paula G. De Pinho , Portugal

Damião De Sousa , Brazil

Francisco Javier Deive , Spain

Tianlong Deng , China



Fatih Deniz , Turkey  
Claudio Di Iaconi, Italy  
Irene Dini , Italy  
Daniele Dondi, Italy  
Yingchao Dong , China  
Dennis Douroumis , United Kingdom  
John Drexler, USA  
Qizhen Du, China  
Yuanyuan Duan , China  
Philippe Dugourd, France  
Frederic Dumur , France  
Grégory Durand , France  
Mehmet E. Duru, Turkey  
Takayuki Ebata , Japan  
Arturo Espinosa Ferao , Spain  
Valdemar Esteves , Portugal  
Cristina Femoni , Italy  
Gang Feng, China  
Dieter Fenske, Germany  
Jorge F. Fernandez-Sanchez , Spain  
Alberto Figoli , Italy  
Elena Forte, Italy  
Sylvain Franger , France  
Emiliano Fratini , Italy  
Franco Frau , Italy  
Bartolo Gabriele , Italy  
Guillaume Galliero , France  
Andrea Gambaro , Italy  
Vijay Kumar Garlapati, India  
James W. Gauld , Canada  
Barbara Gawdzik , Poland  
Pier Luigi Gentili , Italy  
Beatrice Giannetta , Italy  
Dimosthenis L. Giokas , Greece  
Alejandro Giorgetti , Italy  
Alexandre Giuliani , France  
Elena Gomez , Spain  
Yves Grohens, France  
Katharina Grupp, Germany  
Luis F. Guido , Portugal  
Maolin Guo, USA  
Wenshan Guo , Australia  
Leena Gupta , India  
Muhammad J. Habib, USA  
Jae Ryang Hahn, Republic of Korea

Christopher G. Hamaker , USA  
Ashanul Haque , Saudi Arabia  
Yusuke Hara, Japan  
Naoki Haraguchi, Japan  
Serkos A. Haroutounian , Greece  
Rudi Hendra , Indonesia  
Javier Hernandez-Borges , Spain  
Miguel Herrero, Spain  
Mark Hoffmann , USA  
Hanmin Huang, China  
Doina Humelnicu , Romania  
Charlotte Hurel, France  
Nenad Ignjatović , Serbia  
Ales Imramovsky , Czech Republic  
Muhammad Jahangir, Pakistan  
Philippe Jeandet , France  
Sipak Joyasawal, USA  
Sławomir M. Kaczmarek, Poland  
Ewa Kaczorek, Poland  
Mostafa Khajeh, Iran  
Srećko I. Kirin , Croatia  
Anton Kokalj , Slovenia  
Sevgi Kolaylı , Turkey  
Takeshi Kondo , Japan  
Christos Kordulis, Greece  
Ioannis D. Kostas , Greece  
Yiannis Kourkoutas , Greece  
Henryk Kozłowski, Poland  
Yoshihiro Kudo , Japan  
Avvaru Praveen Kumar , Ethiopia  
Dhanaji Lade, USA  
Isabel Lara , Spain  
Jolanta N. Latosinska , Poland  
João Paulo Leal , Portugal  
Woojin Lee, Kazakhstan  
Yuan-Pern Lee , Taiwan  
Matthias Lein , New Zealand  
Huabing Li, China  
Jinan Li , USA  
Kokhwa Lim , Singapore  
Teik-Cheng Lim , Singapore  
Jianqiang Liu , China  
Xi Liu , China  
Xinyong Liu , China  
Zhong-Wen Liu , China

Eulogio J. Llorent-Martínez , Spain  
Pasquale Longo , Italy  
Pablo Lorenzo-Luis , Spain  
Zhang-Hui Lu, China  
Devanand Luthria, USA  
Konstantin V. Luzyanin , United Kingdom  
Basavarajaiah S M, India  
Mari Maeda-Yamamoto , Japan  
Isabel Mafra , Portugal  
Dimitris P. Makris , Greece  
Pedro M. Mancini, Argentina  
Marcelino Maneiro , Spain  
Giuseppe F. Mangiatordi , Italy  
Casimiro Mantell , Spain  
Carlos A Martínez-Huitle , Brazil  
José M. G. Martinho , Portugal  
Andrea Mastinu , Italy  
Cesar Mateo , Spain  
Georgios Matthaiolampakis, USA  
Mehrab Mehrvar, Canada  
Saurabh Mehta , India  
Oinam Romesh Meitei , USA  
Saima Q. Memon , Pakistan  
Morena Miciaccia, Italy  
Maurice Millet , France  
Angelo Minucci, Italy  
Liviu Mitu , Romania  
Hideto Miyabe , Japan  
Ahmad Mohammad Alakraa , Egypt  
Kaustubha Mohanty, India  
Subrata Mondal , India  
José Morillo, Spain  
Giovanni Morrone , Italy  
Ahmed Mourran, Germany  
Nagaraju Mupparapu , USA  
Markus Muschen, USA  
Benjamin Mwashote , USA  
Mallikarjuna N. Nadagouda , USA  
Lutfun Nahar , United Kingdom  
Kamala Kanta Nanda , Peru  
Senthilkumar Nangan, Thailand  
Mu. Naushad , Saudi Arabia  
Gabriel Navarrete-Vazquez , Mexico  
Jean-Marie Nedelec , France  
Sridhar Goud Nerella , USA  
Nagatoshi Nishiwaki , Japan  
Tzortzis Nomikos , Greece  
Beatriz P. P. Oliveira , Portugal  
Leonardo Palmisano , Italy  
Mohamed Afzal Pasha , India  
Dario Pasini , Italy  
Angela Patti , Italy  
Massimiliano F. Peana , Italy  
Andrea Penoni , Italy  
Franc Perdih , Slovenia  
Jose A. Pereira , Portugal  
Pedro Avila Pérez , Mexico  
Maria Grazia Perrone , Italy  
Silvia Persichilli , Italy  
Thijs A. Peters , Norway  
Christophe Petit , France  
Marinos Pitsikalis , Greece  
Rita Rosa Plá, Argentina  
Fabio Polticelli , Italy  
Josefina Pons, Spain  
V. Prakash Reddy , USA  
Thathan Premkumar, Republic of Korea  
Maciej Przybyłek , Poland  
María Quesada-Moreno , Germany  
Maurizio Quinto , Italy  
Franck Rabilloud , France  
C.R. Raj, India  
Sanchayita Rajkhowa , India  
Manzoor Rather , India  
Enrico Ravera , Italy  
Julia Revuelta , Spain  
Muhammad Rizwan , Pakistan  
Manfredi Rizzo , Italy  
Maria P. Robalo , Portugal  
Maria Roca , Spain  
Nicolas Roche , France  
Samuel Rokhum , India  
Roberto Romeo , Italy  
Antonio M. Romerosa-Nievas , Spain  
Arpita Roy , India  
Eloy S. Sanz P rez , Spain  
Nagaraju Sakkani , USA  
Diego Sampedro , Spain  
Shengmin Sang , USA

Vikram Sarpe , USA  
Adrian Saura-Sanmartin , Spain  
St phanie Sayen, France  
Ewa Schab-Balcerzak , Poland  
Hartwig Schulz, Germany  
Gulaim A. Seisenbaeva , Sweden  
Serkan Selli , Turkey  
Murat Senturk , Turkey  
Beatrice Severino , Italy  
Sunil Shah Shah , USA  
Ashutosh Sharma , USA  
Hideaki Shirota , Japan  
Cl udia G. Silva , Portugal  
Ajaya Kumar Singh , India  
Vijay Siripuram, USA  
Ponnurengam Malliappan Sivakumar ,  
Japan  
Tom s Sobrino , Spain  
Raquel G. Soengas , Spain  
Yujiang Song , China  
Olivier Soppera, France  
Radhey Srivastava , USA  
Vivek Srivastava, India  
Theocharis C. Stamatatos , Greece  
Athanasios Stavrakoudis , Greece  
Darren Sun, Singapore  
Arun Suneja , USA  
Kamal Swami , USA  
B.E. Kumara Swamy , India  
Elad Tako , USA  
Shoufeng Tang, China  
Zhenwei Tang , China  
Vijai Kumar Reddy Tangadanchu , USA  
Franco Tassi, Italy  
Alexander Tatarinov, Russia  
Lorena Tavano, Italy  
Tullia Tedeschi, Italy  
Vinod Kumar Tiwari , India  
Augusto C. Tome , Portugal  
Fernanda Tonelli , Brazil  
Naoki Toyooka , Japan  
Andrea Trabocchi , Italy  
Philippe Trens , France  
Ekaterina Tsipis, Russia  
Esteban P. Urriolabeitia , Spain


Toyonobu Usuki , Japan  
Giuseppe Valacchi , Italy  
Ganga Reddy Velma , USA  
Marco Viccaro , Italy  
Jaime Villaverde , Spain  
Marc Visseaux , France  
Balaga Viswanadham , India  
Alessandro Volonterio , Italy  
Zoran Vujcic , Serbia  
Chun-Hua Wang , China  
Leiming Wang , China  
Carmen W ngler , Germany  
Wieslaw Wiczkowski , Poland  
Bryan M. Wong , USA  
Frank Wuest, Canada  
Yang Xu, USA  
Dharmendra Kumar Yadav , Republic of  
Korea  
Maria C. Yebra-Biurrun , Spain  
Dr Nagesh G Yernale, India  
Tomokazu Yoshimura , Japan  
Maryam Yousaf, China  
Sedat Yurdakal , Turkey  
Shin-ichi Yusa , Japan  
Claudio Zaccone , Italy  
Ronen Zangi, Spain  
John CG Zhao , USA  
Zhen Zhao, China  
Antonio Zizzi , Italy  
Mire Zloh , United Kingdom  
Grigoris Zoidis , Greece  
Deniz  AHİN , Turkey



## Contents


---

**New Online Shunt Acidification for Water Injection Increasing Technology and Its Application in Huanjiang Oilfield**

Zhiying Deng , Zhenning Ji, Suiwang Zhang, Lingpu He, Xiaobing Lu, Wenchao Wu, Liwei Xiong, and Haiming Fan 

Research Article (7 pages), Article ID 3989308, Volume 2021 (2021)

**3D Physical Simulation Experiment of Edge Water Reservoir by Polymer/Surfactant Binary Flooding**

Qunyi Wang, Wenshuang Geng , Fuquan Luo, Changcheng Gai, Xuena Zhang, and Xiao Gu

Research Article (9 pages), Article ID 7932381, Volume 2020 (2020)

## Research Article

# New Online Shunt Acidification for Water Injection Increasing Technology and Its Application in Huanjiang Oilfield

Zhiying Deng <sup>1,2,3</sup>, Zhenning Ji,<sup>2,3</sup> Suiwang Zhang,<sup>2,3</sup> Lingpu He,<sup>4</sup> Xiaobing Lu,<sup>2,3</sup> Wenchao Wu,<sup>5</sup> Liwei Xiong,<sup>1</sup> and Haiming Fan <sup>6</sup>

<sup>1</sup>Hubei Key Laboratory of Plasma Chemistry and Advanced Materials, Wuhan Institute of Technology, Wuhan 430205, China

<sup>2</sup>National Engineering Laboratory for Exploration and Development of Low-permeability Oil and Gas Field, Xi'an 710018, China

<sup>3</sup>Oil & Gas Technology Research Institute of Changqing Oil Field Company, Xi'an 710018, China

<sup>4</sup>The 4th Oil Production Plant of Changqing Oil Field Company, Yinchuan 750000, China

<sup>5</sup>Shanxi Ming De Petroleum Technology Limited Company, Xi'an 710018, China

<sup>6</sup>Shandong Key Laboratory of Oilfield Chemistry, School of Petroleum Engineering, China University of Petroleum (East China), Qingdao 266580, Shandong, China

Correspondence should be addressed to Zhiying Deng; [fhmwd@163.com](mailto:fhmwd@163.com)

Received 20 June 2020; Accepted 2 September 2021; Published 10 December 2021

Academic Editor: Kaustubha Mohanty

Copyright © 2021 Zhiying Deng et al. This is an open access article distributed under the Creative Commons Attribution License, which permits unrestricted use, distribution, and reproduction in any medium, provided the original work is properly cited.

The poor physical property and strong heterogeneity of Triassic Yanchang formation in Huanjiang oilfield of Ordos Basin are the main reasons for uneven water absorption, partial injection wells underinjection at high pressure, and decline of production. Previously, large numbers of conventional acidifications were used for plugging removal in the reservoir, but the effect was not so good and effective period was short. Aiming at the geological characteristics of Huanjiang oilfield, an online shunt acidification and augmented injection technology which does not stop water injection, pull original production strings out, and continuously inject acid and diverting agent has been proposed. A chelating acid COA-1S with low corrosion rate (0.3675 g/(m<sup>2</sup>·h)), good retardation capacity (hydrolysis constant = 1.2 × 10<sup>-6</sup>), and effective chelating ability (precipitation inhibition rate >95%) has been developed, as well as a diverting agent COA-1P with good dispersion in acid solution, diversion effect, and particle size (10–100 μm), which behaves well in COA-1S acid. It has been proved that the online acid system has a good diversion acidizing ability and plugging removal performance in a deep area in the laboratory core physical simulation test. The field test results show that the online shunt acidizing and augmented injection technology could reduce the injection pressure significantly (4.2 MPa) and increase water injection by 10 m<sup>3</sup>/d for the measured well (H5) and improve the water injection profile prominently. The online shunting acidification and augmented injection technology have the following advantages: simple procedures, fewer equipment needed, high efficiency of depressurization, and increasing water injection, which could effectively improve the profile of water wells, and there is a bright future of the technology.

## 1. Introduction

The main development layer of Huanjiang oilfield is the Triassic Yanchang formation, the average porosity of the reservoir is 10.9%, and the average permeability is 0.43 × 10<sup>-3</sup> μm<sup>2</sup>, so Huanjiang oilfield belongs to the ultra-low-permeability sandstone reservoir. Due to poor physical properties of the reservoir and injected water not up to standard, as well as other

reasons, many problems such as uneven water absorption, increasing water injection pressure, and more and more injecting wells underinjection have arisen. In recent years, aiming at the problem of underinjection of Huanjiang oilfield, a series of measures have been carried out to reduce water injection pressure and increase water injection and have achieved great efforts; however, the effective period of these measures is short (average 79 days) and effective rate is low (average 73%).

The main reasons are as follows: (1) because of the repeated acidification of wells, the damaging radius is getting bigger; (2) after acidification, the acid solution produced secondary damage and caused secondary blockage to the reservoir, and (3) due to strong heterogeneity of the reservoir, acid absorption of different layers varies and low-permeability layers absorb fewer acid, resulting in poor acidification effect [1].

Based on the geological characteristics of Huanjiang oilfield, an online shunt acidification and augmented injection technology with not stopping water injection, not pulling out the original production strings, and continuous injection of acid have been proposed. The field test results showed that the technology behaves well, which could greatly reduce the water injection, improve the water injection volume, and effectively improve the profile of the wells. It has a good application prospect, and there is a bright future of the technology [2, 3].

## 2. Analysis of the Theory and Adaptability of Online Diversion Acidification

**2.1. Shunt Acidizing Theory.** Generally, acid flows through the small layers linearly should obey Darcy law. In order to make the acid move into the per small layer (or small section) and reach the goal of plugging removal in each layer (section) proportionately, it must obey the rule that the acid injection rate on per unit area of small layers (or small section) is the same [4], which means it should meet the following relation:

$$\frac{K_1 \Delta P_1}{\mu_1 L_1} = \frac{K_2 \Delta P_2}{\mu_2 L_2} = \dots = \frac{K_i \Delta P_i}{\mu_i L_i} = \dots = \frac{K_N \Delta P_N}{\mu_N L_N} \quad (1)$$

In the relation,  $K$ - permeability,  $10^{-3} \mu\text{m}^2$ ;  $\Delta P$ - pressure difference, MPa;  $\mu$ - injection viscosity, mPa·s;  $L$ - distance of pressure differential, m<sup>3</sup>; and  $N$ - total amount of layers.

Due to the affect of damage degree, reservoir pressure, fluid compressibility, fluid viscosity, and natural seam hole development of small layers (or small section) [5], when measures are not taken, the relation is not met; therefore, temporary plugging or shunt technology should be considered.

The online shunt acidification is an injection process which does not need to pull the original pipes out during acidification; meanwhile, acid and diverting agent are injected together with water. In the early stage, the acid prefers to enter the high-permeability layer, as the effect of the diverting agent, permeability of high permeability layer would decrease with increase entering of diverting agent, therefore, the subsequent acid would rather enter other layers with low permeability, and finally, the goal of acid entering into all layers proportionally is achieved [6].

**2.2. Performance Evaluation of Chelating Acid.** Chelate acid (COA-1S) is a kind of multivariant organic acid, with 24 O<sup>2-</sup>, 12 OH<sup>-</sup> and 6 PO<sub>3</sub><sup>-</sup>, and N and O heteroatoms which contain unshared electron pairs with the greater electro-negativity, and when the groups encounter Ca<sup>2+</sup>, Ba<sup>2+</sup>, Sr<sup>2+</sup>, Fe<sup>3+</sup>, and other high-valence metal cations, stable complexes

are easily generated, which are very stable in the wide range of pH value [7]. Table 1 shows the chelating performance of the acid solution. It can be seen that compared with mud acid and multihydrogen acid, chelate acid (COA-1S) is superior in inhibiting precipitation, with the pH value of the solution increased from 3 to 7, the precipitation inhibition rate of COA-1S to Ba<sup>2+</sup> increases rapidly, indicating the increase of pH value caused by acid consumption does not reduce chelating ability, and the resulting complex are stable enough to prevent the secondary precipitate.

The hydrolysis equilibrium constant of chelate acid (COA-1S) is only about  $1.2 \times 10^{-6}$ ; therefore, the concentration of chelating acid is very low when hydrolysis equilibrium is reached, and the hydrolysis reaction process is slow. In the process of acidizing and plugging removal, in order to maintain the equilibrium of hydrolysis, the ionized H<sup>+</sup> generally reacts with sandstone minerals, thus slowing down the reaction rate of acid and rock and achieving the goal of plugging removal in the deep area. Comparing with conventional mud acid, the superior performance in retardation of COA-1S provides a guarantee for improving the acidification effect in the deep area.

Referring to the SY/T 5405-1996 "Performance test method and evaluation index of corrosion inhibitor for acidification," the corrosion rate of COA-1S (50%) for N80 steel sheet and tube column coated is determined under 60°C, and the corrosion rates are 0.2895 g/(m<sup>2</sup>·h) and 0.3675 g/(m<sup>2</sup>·h), respectively, and the results are only 10% of the industry standard level (3.0 g/(m<sup>2</sup>·h), which indicates that COA-1S has less corrosion to inner tubes, and the pictures of steel sheets before and after corrosion tests (shown in Figure 1) also support the standpoint.

**2.3. Performance Evaluation of the Diverting Agent.** The diverting agent COA-1P is a kind of salt substance, which is a colorless transparent liquid with a density of 1.07 g/cm<sup>3</sup>. Figure 2 shows solubility evaluation results of the diverting agent. It can be seen that the solution is clear and transparent when diverting agent COA-1P mixes with tap water, and when mixing diverting agent COA-1P with the chelate acid COA-1S, uniform and dispersed white small particles are produced. With the increase in the amount of tap water, the pH value of the solution increases gradually, and the white particles gradually dissolve and are completely dissolved when the pH value is 7. During onsite operation, firstly, the chelate acid COA-1S should be injected into the formation to remove pollution in the zone; secondly, the diverting agent is added to produce chemical particles to form temporary plugging; thirdly, chelate acid COA-1S is injected again to be forced to flow to the low-permeability zone, aiming at improving the longitudinal water absorption section of water injection wells; finally, the normal water injection is recovered to relieve the blockage of the diverting agent to the high-permeability zone.

In order to fully understand the distribution of the particle size of the diverting agent COA-1P in the acid solution, the particle size distribution of COA-1S and COA-1P mixed solution with different concentration is detected



TABLE 1: The chelating performance of chelate acid COA-1S and other acids.

Sample	Scale inhibition rate to BaSO <sub>4</sub> (%)				Inhibition rate (%)		
	pH=3	pH=5	pH=6	pH=7	CaF <sub>2</sub>	Fe(OH) <sub>3</sub>	Fluoroaluminate
Mud acid	0.73	0.76	0.79	0.68	—	—	—
Multihydrogen acid	3.41	5.58	7.39	9.38	60.72	36.26	31.45
COA-1S	15.62	64.37	78.69	89.37	98.81	96.62	96.72

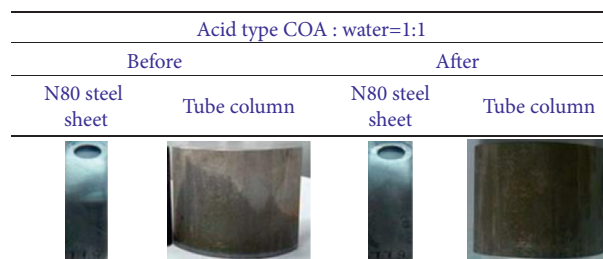


FIGURE 1: Pictures before and after corrosion tests of steel sheets.

by using a laser particle size analyzer. The results are shown in Table 2. It can be seen from Table 2 that the resulting white particle size is mainly from 10 to 100  $\mu\text{m}$ , and the pore throat of the target reservoir is mainly from 0.22 to 33.82  $\mu\text{m}$ . Therefore, the size of the particle could be changed by adjusting the concentration of the acid liquid and the diverting agent, so as to achieve the purpose of blocking the high-permeability layer temporarily and meet the shunting requirements [8, 9].

**2.4. Compatibility Evaluation.** The compatibility tests for the chelate acid COA-1S and diverting agent COA-1P with injected water and formation water are carried out under the conditions of 20 and 60°C, respectively. The results show that the compatibility of the two liquids with injected water and the formation water is good at different temperatures.

### 3. Simulation Experiment Research of Online Shunt Acidification Experiment

In order to further verify the feasibility of the technology, parallel core flow tests are carried out using two cores with different permeabilities selected from the corresponding reservoirs in Huanjiang oilfield [10, 11], and the effects of shunt and acidification are analyzed. The experiment temperature is 60°C, and the experiment apparatus is the multifunctional shunt acidification experiment instrument which is self-developed. The results are shown in Figure 3 and Table 3.

Figure 3 is the pressure variation curve of the core of the H2 well after injecting acid and diverting agent. It can be seen that the pressure of core 1 changed little and the pressure of core 2 dropped after injecting 50% COA-1S acid, indicating that acid is mainly injected into core 2. After the injection of 6% COA-1P, the pressure of the two cores fluctuate greatly, and the pressure increases with the diverting agent and acid injecting sequentially, which indicate that the COA-1P played a temporary plugging role.

The pressure drops sharply with injection of stratum water after the acid liquid, which shows that COA-1P is dissolved by water and it does not plug the formation during the normal water injection.

Table 3 shows the results of permeability before and after the shunt acidification tests. It can be seen that the permeability of core 1 and 2 increase by 10.5 and 3.1 times, respectively, indicating that the diverting agent has effectively plugged core 2 and both the two cores have been completely acidified, and the effect of shunt acidification is good.

## 4. Field Application Example

**4.1. Basic Situation and Analysis of Site Operation.** On October 15, 2017, the onsite operation of online shunt acidification in well H5 of Huanjiang oilfield was carried out (shown in Figure 4), the dosage of shunt agent COA-1P was 2 m<sup>3</sup>, and the dosage of chelate acid was 17.4 m<sup>3</sup>. The operation procedures are as follows: (1) Pressure test and water squeeze. (2) The first stage of acid COA-1S was injected into the formation to remove reservoir choke and reduce the water injection pressure. The operation flow rate was 1.0 m<sup>3</sup>/h–3.0 m<sup>3</sup>/h, and the ratio of acid COA-1S to injected water was 1 : 1.5. The cumulative injection volume was 12 m<sup>3</sup>, of which 4.8 m<sup>3</sup> acid liquid was squeezed from the well test valve to the reservoir, and the rest was injected from the normal process to the reservoir. (3) The second stage mixed solution of acid COA-1S and shunt COA-1P was injected into the formation, the flow rate of diverting agent was 1.0 m<sup>3</sup>/h, and the injection volume of diverting agent was 2 m<sup>3</sup>; while the flow rate of acid solution was 1.2 m<sup>3</sup>/h, and the cumulative injection volume of acid solution was 2.4 m<sup>3</sup>. (4) The third stage acid solution was injected into the formation. The operation flow rate was 1.2–3.0 m<sup>3</sup>/h, and the ratio of acid COA-1S to injected water was 1 : 1, 10.2 m<sup>3</sup> of acid liquid was squeezed from the oil pipe to the reservoir, and the other 10.2 m<sup>3</sup> of water was injected from the distribution room to the casing pipe. (5) The water injection

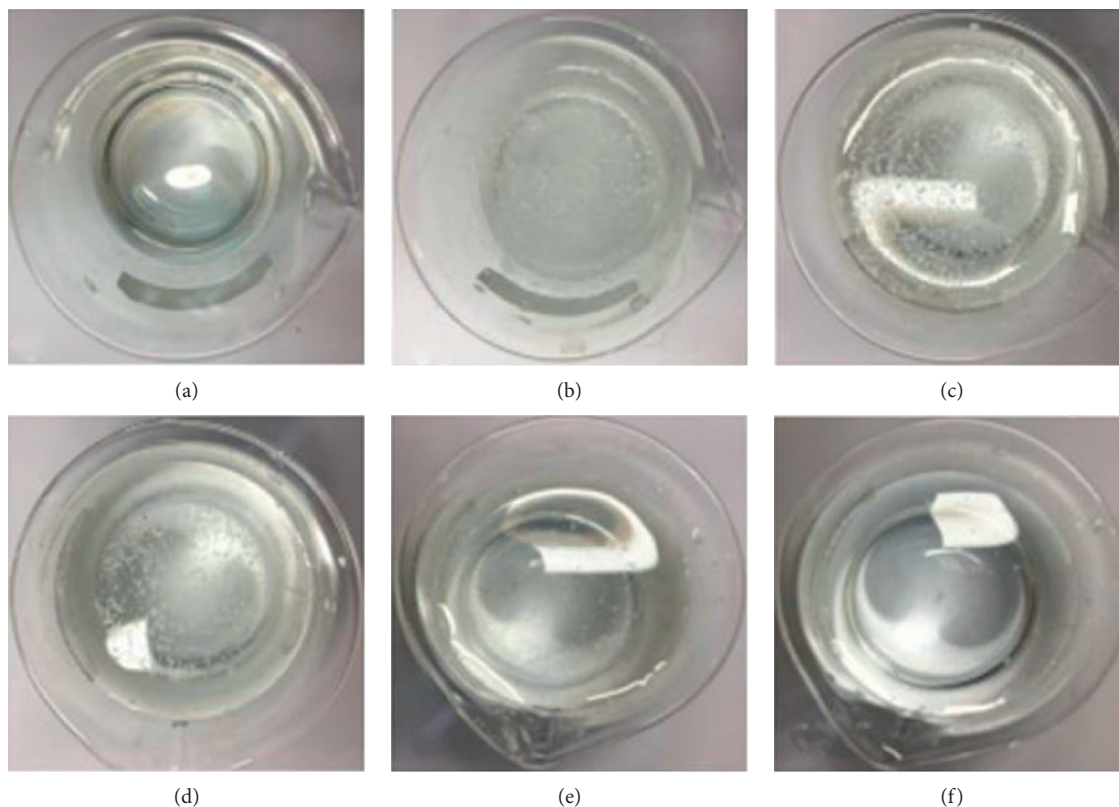


FIGURE 2: The solubility of water-soluble white particles. (a) Diverting agent + tap water; (b) diverting agent+10 ml of chelate acid; (c) 100 ml of fresh water is added for the first time, pH<1; (d) 300 ml of fresh water is added for the second time, pH = 4; (e) 500 ml of fresh water is added for the third time, pH = 5; and (f) 1000 ml of fresh water is added for the fourth time, pH = 7.

TABLE 2: Particle size distribution of the mixed solution of COA-1P and COA-1S.

Group	COA-1P concentration (%)	COA-1S concentration (%)	pH	Particle size ( $\mu\text{m}$ )		
				$d$ (0.1)	$d$ (0.5)	$d$ (0.9)
1	5	5	<1	13.88	41.48	107.00
2	10	10	<1	15.73	42.43	110.12
3	10	—	3	11.16	38.34	102.36
4	10	—	5	10.54	38.24	100.45

process was recovered. The water injection pressure was 16.5 MPa, and the instantaneous flow rate was  $1.0 \text{ m}^3/\text{h}$ .

The operation curve is shown in Figure 5. It can be seen that, (1) when the sleeve valve was open, the acid liquid was squeezed into the formation and the pressure rose, indicating that it was difficult for the formation to absorb the water. (2) In the process of acid injection under high pressure, the operation pressure increased from 15.3 MPa to 17.3 MPa after the acid entered the well bottom, which indicated that the diverting agent played an effective role in plugging the high permeability layer. (3) At the end of acidification, the pressure of was 16.5 MPa after the injection pump was stopped. After recovering the water injection process, the water injection pressure decreased from 17.3 to 16.5 MPa. At present, the injection pressure was 14.9 MPa, which dropped 4.2 MPa comparing with not operated before, indicating that the effect of acid liquid for plugging

removal was obvious. (4) From 14:29 to 2:57, the whole construction cycle which was reduced at least 1 to 7 times was less than 13 hours, compared with the conventional profile adjustment technology for more than 7 days. In the process of acidification operation, there were no need of leakage of the water in the tube, pulling the original pipes out, changing acid, and flowback of the residual liquor. Online shunt acidizing technology greatly simplified the conventional acidification process and shortened the operation period. Moreover, in contrast to the soil pollution caused by the conventional profile adjustment technology, which needed to drain water and regurgitate reacted acid to the ground, it reduced the risk of safety and environmental pollution. Last, during the conventional profile adjustment construction, the well must be off when tripping operation and changing acid, but water and acid mixed liquid could be injected at the same time, and the original injection process

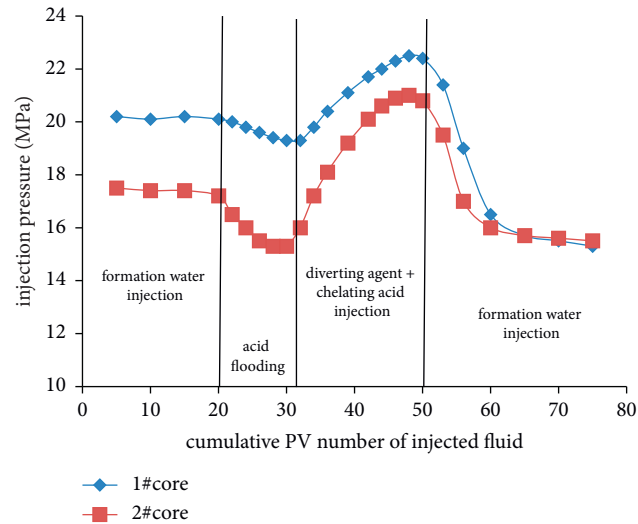


FIGURE 3: The curve of pressure of change of the core of the H2 well.

TABLE 3: Experimental results of H2 core diversion acidification.

Core number	Depth (m)	Initial permeability ( $10^{-3} \mu\text{m}^2$ )	Permeability after diversion acidification ( $10^{-3} \mu\text{m}^2$ )	Permeability increasing multiple
1	2631.4	0.12	1.26	10.5
2	2640.3	0.64	1.98	3.1

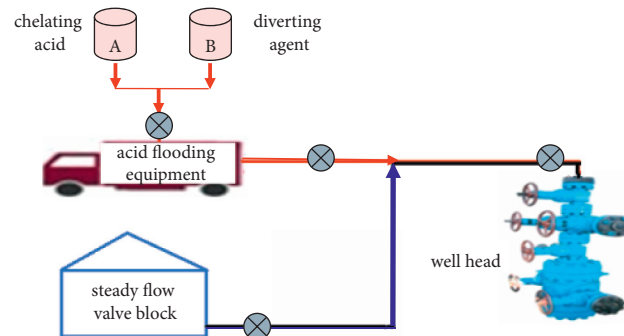


FIGURE 4: Flow chart of the online diversion acidizing operation process.

would not be stopped, which did not affect the normal water injection of water injection wells in the process of online shunt acidizing.

**4.2. Profile Adjustment.** Figure 6 shows the variation of the water absorption profile before and after the online shunt acidification of the H5 well. It can be seen that the upside of operated wells (2628–2638 m) absorbed water weakly and the lower section of wells (2638–2643 m) showed obvious characteristics of water absorption. The maximum water absorption intensity was  $3.47 \text{ m}^3/\text{d}\cdot\text{m}$ , and the degree of water absorption was only 28.5%. After the online shunt acidification, the upper and lower section of wells absorbed balanced water amount, the average water absorption intensity was  $1.42 \text{ m}^3/\text{d}\cdot\text{m}$ , and the degree of water absorption was 50.9%. The results demonstrated that the online shunt

acidification could achieve well-proportioned acid distribution and improve the water absorption profile of the operated well effectively.

**4.3. Effect of Depressurization and Injection Augment.** Figure 7 shows the water injection curve before and after online shunt acidification of the H5 well. Before acidification, the oil pressure was 19.1 MPa, the allocation injection amount of water was  $25 \text{ m}^3/\text{d}$ , and the actual water injection amount was  $15 \text{ m}^3/\text{d}$ . After acidification, the oil pressure was 14.9 MPa, the allocation injection amount of water was  $25 \text{ m}^3/\text{d}$ , and the actual daily injection amount was  $25 \text{ m}^3/\text{d}$ . The water absorption index increased two times as before, and the effect of decrease of pressure and increase water injection was obvious.



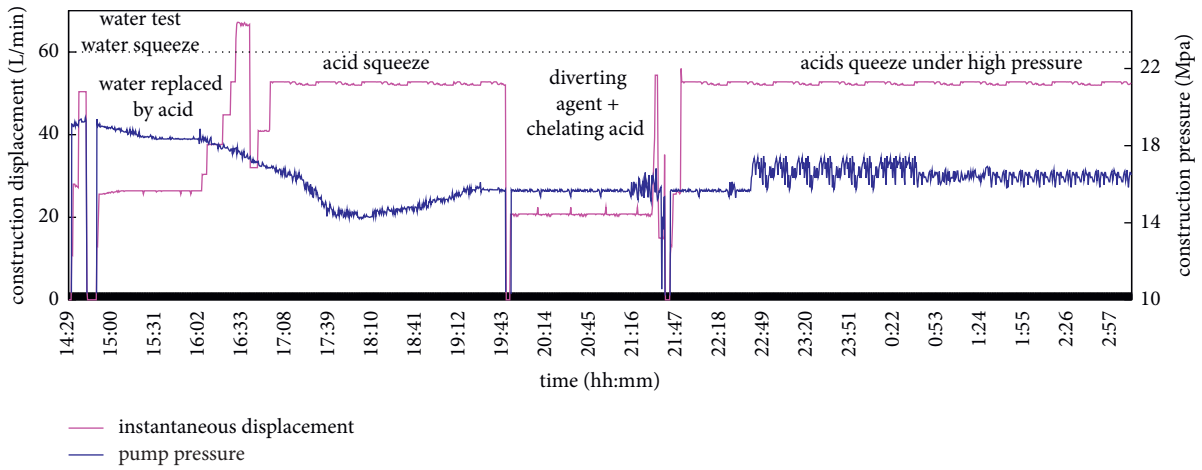


FIGURE 5: The operation curve of the online diversion acidification of the H5 well.

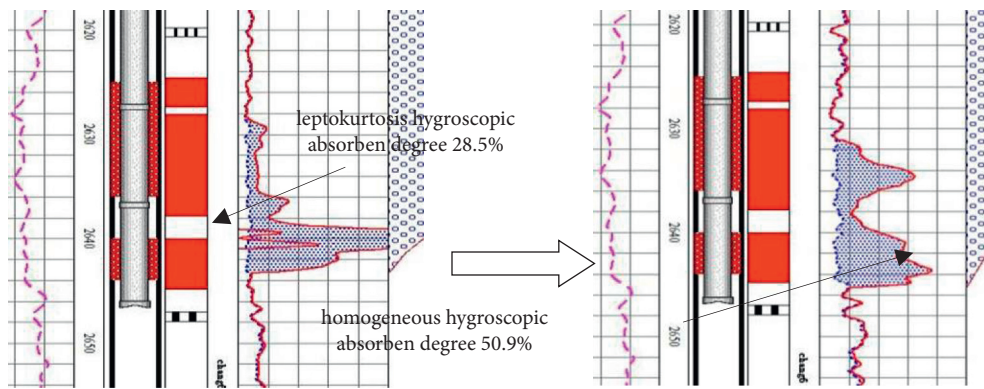


FIGURE 6: Absorption profile of the H5 well.

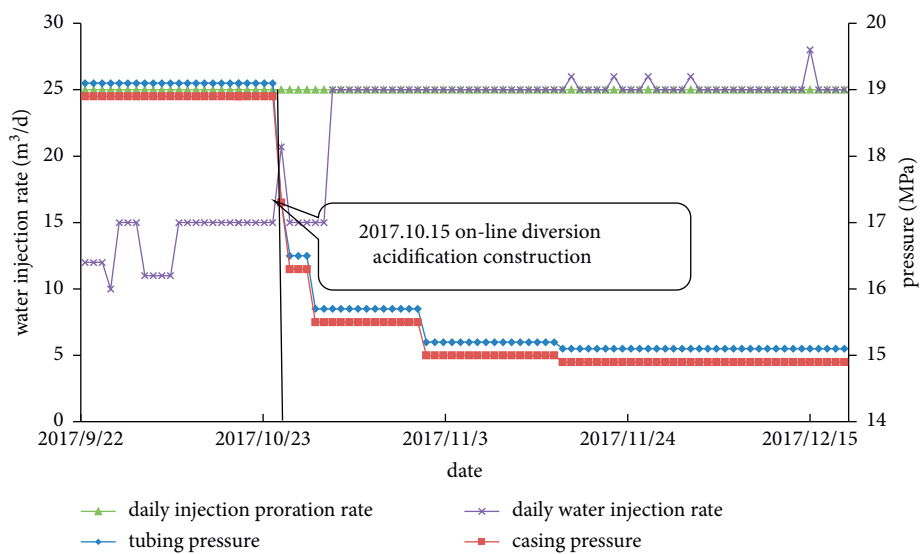


FIGURE 7: The water injection curve of the H5 well before and after online diversion acidification.

## 5. Conclusions

- (1) Compared with conventional mud acid and multi-hydrogen acid, chelate acid COA-1S is superior in corrosion rate, retardation capacity, and chelating ability, which could slow down acidification rate, increase the time of operation, prolong acidification distance, reduce secondary precipitation of barium and strontium, and improve the effect of acidification.
- (2) The water-soluble diversion agent COA-1P could produce chemical particles when in contact with acid liquid and can make the proportional distribution of acid in the objective layer and improve the utilization of acid liquid, as well as the longitudinal water absorption profile of wells underinjection. Moreover, the diversion agent COA-1P could completely dissolve in the formation water and the injected water, which did not cause secondary plugging to the formation.
- (3) The online shunt acidification augmented injection technology was successfully applied in the H5 well of Huanjiang oilfield. It is proved that the technology had good applicability for the similar reservoirs and had important significance for improving the effect of water injection in similar oilfields.
- (4) Based on the different blockage reasons of each block of the ultra-low-permeability reservoir in Huanjiang Oilfield, the continuous injection online diversion acidification technology will act as the main part, with different other injection parts, such as inhibiting scale part and preventing clay swelling part and nanoaugmented injection, forming a set of online injection process systems, to solve the problems of high-pressure water wells underinjection in ultra-low-permeability reservoirs effectively.

## Data Availability

The data used to support the findings of this study are included within the article.

## Conflicts of Interest

The authors declare no conflicts of interest regarding the publication of this paper.

## Acknowledgments


This work was financially supported by the National Natural Science Foundation of China (51402220), Key Project of Hubei Education Department (D20191503), and Wuhan Institute of Technology Science Foundation (K201801).

## References

- [1] W. Chen, X. F. Yuan, and J. C. Guo, "Application and evaluation on multi-hydro acid deep diversion acidizing technology in Donghe oil-field," *Chemical Engineering of Oil & Gas*, vol. 40, pp. 285–288, 2011.
- [2] X. Liu, L. Q. Zhao, Z. Yang, and Y. G. Liu, "Application of acidizing technology with original production string in bohái oilfield," *Oil Drilling & Production Technology*, vol. 26, pp. 47–49, 2004.
- [3] Y. Fan and M. J. Economides, "Fracturing fluid leakoff and net pressure behavior," in *Proceedings of the Frac & Pack Stimulation, Society of Petroleum Engineers of AIME*, Article ID 29988, Beijing, China, November 1995.
- [4] P. Y. Gao, P. L. Liu, H. Liu, X. H. Meng, J. C. Gao, and S. Y. Fu, "Research on water soluble micro-particle diverting agent SA-2," *DFCF*, vol. 29, pp. 67–70, 2012.
- [5] P. L. Liu, Y. G. Liu, L. Q. Zhao, and J. M. Chen, "Study and application on acidizing high permeability & high porosity reservoir in Bohai bay oil-field," *Journal of Southwest Petroleum Institute*, vol. 27, pp. 52–56, 2005.
- [6] N. Water, L. Jairo, and M. Aatur, "Multilayered reservoir stimulation: case study of effective acid diversion achieved using the associative polymer treatment diverting agent," in *Proceedings of the Khuff Carbonate Reservoir Wells, Saudi Arabia's Ghawar Field, Society of Petroleum Engineers of AIME*, Article ID 123442, Jakarta, Indonesia, August 2009.
- [7] P. L. Liu, F. Li, X. T. Lan, C. L. Liu, and N. Y. Li, "Development of new self-diverting acid for sandstone reservoirs offshore," *Drilling and Production Technology*, vol. 40, pp. 90–93, 2017.
- [8] M. Liu, S. Zhang, J. Mou, F. Zhou, and Y. Shi, "Diverting mechanism of viscoelastic surfactant-based self-diverting acid and its simulation," *Journal of Petroleum Science and Engineering*, vol. 105, pp. 91–99, 2013.
- [9] L. P. Ma, T. Zhang, L. H. Yang, and L. J. Zheng, "The laboratory research on self diverting acidizing and its application in oilfield," *Offshore Oil*, vol. 40, pp. 90–93, 2017.
- [10] D. Taylor, P. S. Kumar, and D. Fu, "Viscoelastic surfactant based self-diverting acid for enhanced stimulation in carbonate reservoirs," in *Proceedings of the SPE European Formation Damage Conference*, Hague, Netherlands, May 2003.
- [11] S. B. Wang, H. R. Wang, J. C. Guo, and J. Lan, "Research and application of self-diverting mud acid in sandstone reservoir acidizing," *Oilfield Chemistry*, vol. 32, pp. 490–493, 2015.

## Research Article

# 3D Physical Simulation Experiment of Edge Water Reservoir by Polymer/Surfactant Binary Flooding

Qunyi Wang, Wenshuang Geng , Fuquan Luo, Changcheng Gai, Xuena Zhang, and Xiao Gu

Research Institute of Exploration and Development, Jidong Oilfield Company, PetroChina, Tangshan 063004, China

Correspondence should be addressed to Wenshuang Geng; [gengwenshuang@126.com](mailto:gengwenshuang@126.com)

Received 16 March 2020; Revised 23 April 2020; Accepted 27 April 2020; Published 13 May 2020

Guest Editor: Dongying Wang

Copyright © 2020 Qunyi Wang et al. This is an open access article distributed under the Creative Commons Attribution License, which permits unrestricted use, distribution, and reproduction in any medium, provided the original work is properly cited.

To investigate the enhanced oil recovery (EOR) technology by chemical flooding in an edge water reservoir, a 3D physical simulation experimental device for the edge water reservoir was developed, and polymer/surfactant binary flooding experiments were carried out under different edge water energies. In addition, the effect and mechanism of binary flooding on EOR under different edge water energies were comprehensively analyzed. Experimental results show that edge water intrusion considerably affects EOR by binary flooding. The stronger the edge water energy, the worse the effect of EOR by binary flooding. Edge water possibly diluted the concentration of the chemical agent medium that is injected into the reservoir, and the degree of dilution varied in different regions. The dilution region was mainly distributed between the injection wells and edge water. The stronger the edge water energy, the higher the dilution multiple of chemical agent and the greater the recovery loss rate by binary flooding.

## 1. Introduction

Edge water reservoir is widely distributed all over the world. The oil production of active edge water reservoir is one of the most challenging problems in petroleum development. In most of these reservoirs, it is likely to form a large water channeling. This phenomenon, which occurs quickly, leads to a rapid increase in the water content of the reservoir. The inflow of water then limits oil recovery, leading to a significant decline in well production [1–3]. However, if the edge water can be effectively restrained or utilized in time, it can once again become a positive energy to improve the development efficiency [4].

For many years, the influence of polymer blocks on bottom water reservoir development has been systematically studied [5]. In addition, some scholars have studied the injection of chemical agents to block the dominant channels and transfer the oil displacement agent to the uncleaned areas. These reported chemical agents include emulsions, foams, air, nanoparticles, and gels [6–9].

The shallow reservoir of the Jidong Oilfield is a typical medium-high permeability natural water drive reservoir,

with an average porosity of 29% and an average permeability of 494 mD [10–12]. The depth of the reservoir is shallow, between 1500 and 2400 m, the fault block area is small, and the average oil-bearing area is only 0.20 km<sup>2</sup>. There are faults in the reservoir, and some areas are connected with the external natural waters, with a certain amount of edge water energy. Currently, this reservoir is at the ultrahigh watercut stage. The composite water cut is greater than 90%, and the degree of reserve recovery is less than 20%. Hence, enhanced oil recovery (EOR) technologies for this type of a reservoir needs to be investigated [13–16]. As a mature and effective oil recovery technology, chemical flooding has garnered increasing attention [17–19]; however, the invasion of edge water has always been an important factor that reduces the effect of chemical flooding. Hence, it is imperative to explore the oil displacement mechanism of chemical flooding in the edge water reservoir [20–23].

In this study, a three-dimensional (3D) physical simulation experimental device for the edge water reservoir is developed according to an actual reservoir. In addition, by employing 3D physical simulation experiments of the polymer/surfactant binary flooding under three water

energy conditions, i.e., no edge water, weak edge water, and strong edge water, respectively, the EOR mechanism by binary flooding under different edge water energy conditions is comprehensively analyzed.

## 2. Model Research and Experimental Design

**2.1. Model Research.** According to the characteristics of the shallow reservoir of the Jidong Oilfield such as a small oil-bearing area and active edge-bottom water, a set of 3D physical simulation experimental devices for the edge water reservoir is developed on the basis of the actual reservoir parameters. The experimental process is shown in Figure 1. The device consists of a model system, a data acquisition and processing system, an automatic control system, a production metering system, and an auxiliary system. Some water intrusion channels are set outside the 3D model, while the edge water permeation plate is set inside the 3D model, which was composed of filling holes and filter mesh. The edge water is injected by an ISCO pump via the outside water invasion channels, infill holes, and filter mesh. And all of these can support the experimental research on the law of water flooding and chemical flooding under the multidirectional edge water invasion condition.

The main parameters are as follows.

The maximum experimental temperature and maximum experimental pressure are 200°C and 10 MPa, respectively; the internal size of the pressure chamber is 300 × 300 × 200 mm; the number of pressure measuring points is 40; the number of differential pressure measuring points is 30; and the number of resistivity measuring points is 64.

The well network in line drive mode is designed on the basis of the shallow reservoir in the Jidong Oilfield (Figure 2). At the water flooding stage, B1–B5 are production wells, which are driven by edge water energy. At the polymer/surfactant binary flooding stage, B1 and B2 are injection wells and B3–B5 are production wells. To dynamically identify the reservoir fluid distribution during the 3D physical simulation, 36 sets of resistivity probes are set up in the model to monitor the changes of resistivity at different locations as well as development phases (Figure 3). Eighteen sampling ports at different locations are set up to sample formation fluids and analyze the chemical agent concentration.

**2.2. Experimental Materials.** Experimental water is the formation water from the shallow reservoir in the Jidong Oilfield; the type of water is NaHCO<sub>3</sub>; and the total salinity is 1635 mg/L. The experimental oil is the simulated oil from the shallow reservoir in the Jidong Oilfield, the crude oil viscosity is 5.0 mPa·s at 70°C, the surfactant (betaine) solution concentration is 0.5%, the polymer hydrolyzed polyacrylamide (HPAM) concentration is 1500 mg/L, and the molecular weight is 1200 × 10<sup>4</sup>–1600 × 10<sup>4</sup>.

**2.3. Experimental Scheme.** Based on the similarity criterion, the experimental parameters are calculated according to the PV number. For flow rate and permeability, according to

Darcy's law, if other parameters remain unchanged, the flow rate and permeability are reduced by 100 times in equal proportion. On the basis of the reduced flow rate, the prototype and the model are compared to ensure that the PV number of the injected fluid is the same to determine the injection time of the model. The experimental parameters are determined (Table 1), and the experimental scheme is designed as follows:

- (1) The injection rate of edge water flooding is 2.5 mL/min
- (2) When the water cut is up to 98%, the polymer/surfactant binary flooding under different edge water energy conditions should be carried out, as shown in Table 2
- (3) When the polymer/surfactant binary flooding is completed, water flooding is carried out at a rate of 2.5 mL/min until the composite water cut reaches 98%.

It is worth mentioning that, through the numerical simulation part, the intrusion speed of the weak edge water and strong edge water (80 and 500 times, respectively) was determined. By adjusting the relationship between the water body multiple and the bottom-hole flowing pressure drop of the edge water drive, the weak and strong water injection rates were determined. Eventually, the experimental schemes of boundless water chemical flooding, weak edge water chemical flooding, and strong edge water chemical flooding were formed.

## 3. Experimental Results and Analysis

**3.1. Effect of Edge Water on Polymer/Surfactant Binary Flooding.** To examine the effect of edge water on the production effect of polymer/surfactant binary flooding, the oil production under different edge water energy conditions is compared. The data obtained from each experimental stage are summarized in Table 3. Based on the experimental data, the curves of the recovery degree and average water cut curves are shown in Figures 4 and 5, respectively.

It can be drawn from Figures 4 and 5 that the production time of the polymer/surfactant binary flooding with weak edge water is the longest, that without edge water is the second, and that with strong edge water is the shortest. The decrease in the average water cut for the polymer/surfactant binary flooding without edge water is the highest, up to 23.90%, while the corresponding values for the polymer/surfactant binary flooding with weak edge water and strong edge water were similar, i.e., 10.74% and 12.95%, respectively. The degree of recovery for the polymer/surfactant binary flooding without edge water is 9.12%, while the corresponding values for the polymer/surfactant binary flooding with weak edge water and strong edge water are 6.67% and 3.76%, respectively. The development effect of the polymer/surfactant binary flooding without edge water is better than that of the weak edge water, and the effect of binary flooding with weak edge water is better than that with strong edge water.

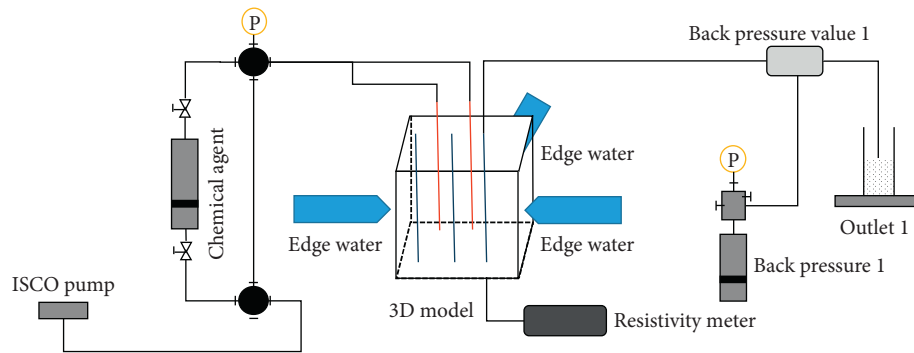


FIGURE 1: Experimental procedure of a high-temperature, high-pressure 3D reservoir simulation system.

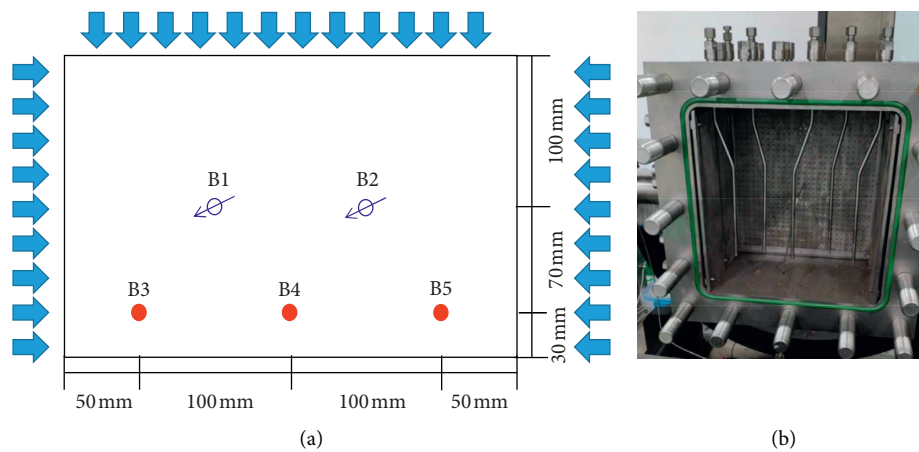


FIGURE 2: Well location of the 3D physical simulation experiment.

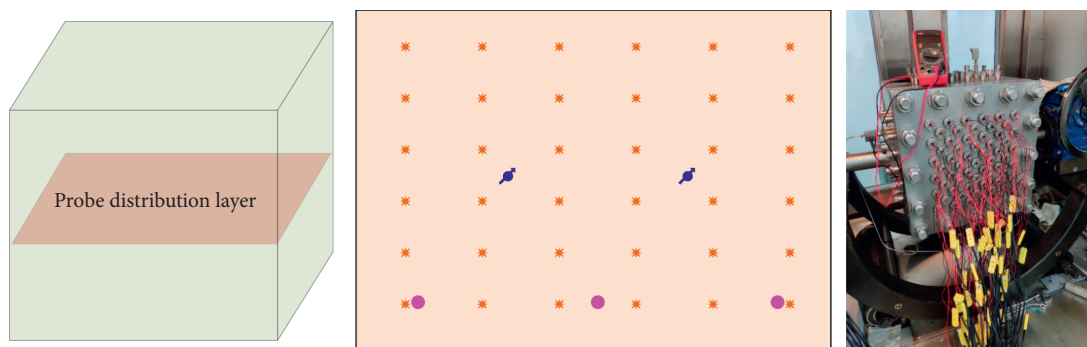


FIGURE 3: Electrode distribution of the 3D physical simulation experiment.

TABLE 1: Experimental parameters.

Items	Reservoir parameters	Experimental parameters
Inclination angle	5°	5°
Effective thickness	5 m	30 cm
Temperature	70°C	70°C
Horizontal permeability	877 mD	3300 mD
Porosity	29%	40%
Injection rate	80 m <sup>3</sup> /d	1.5 mL/min

TABLE 2: Parameters of the displacement experiment scheme.

Number	Experimental scheme	Injection rate of edge water	Injection rate of chemical agent	Liquid production rate
1	Polymer/surfactant binary flooding without edge water	0	1.50 mL/min	1.50 mL/min
2	Polymer/surfactant binary flooding with weak edge water	0.13 mL/min	0.47 mL/min	0.60 mL/min
3	Polymer/surfactant binary flooding with strong edge water	1.00 mL/min	1.50 mL/min	2.50 mL/min

TABLE 3: Production data of each experimental stage.

Parameter design	Polymer/surfactant binary flooding without edge water	Polymer/surfactant binary flooding with weak edge water	Polymer/surfactant binary flooding with strong edge water
Injected PV	0.37 (polymer/surfactant binary flooding without edge water) + 0.39 (following water flooding)	0.34 (polymer/surfactant binary flooding with weak edge water) + 1.15 (following water flooding)	0.29 (polymer/surfactant binary flooding with strong edge water) + 0.51 (following water flooding)
Cumulative production (mL)	677	500	282
Recovery degree (%)	9.12	6.67	3.76

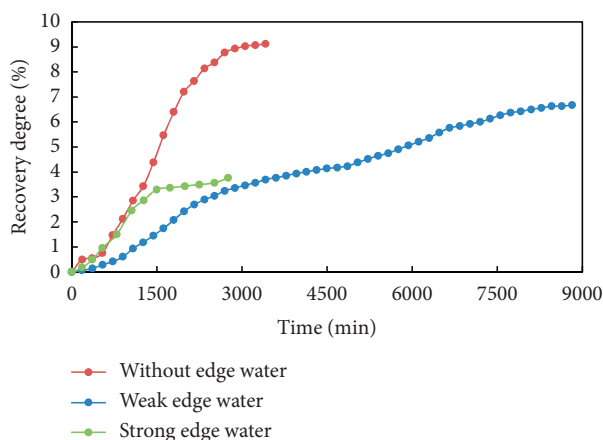


FIGURE 4: Curves of the recovery degree under different edge water energy conditions.

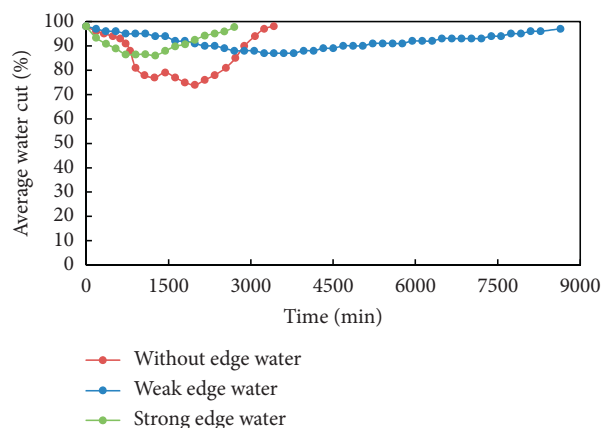


FIGURE 5: Curves of the average water cut under different edge water energy conditions.

3.2. *Effect of Edge Water on the Remaining Oil Saturation during Polymer/Surfactant Binary Flooding.* Figures 6 and 7 show the remaining oil saturation distributions for the polymer/surfactant binary flooding with strong edge water and without edge water, respectively. To more intuitively compare the effects of binary flooding under different edge water energy conditions, the remaining oil saturation of binary flooding with strong edge water is subtracted from that of binary flooding without edge water. Figure 8(a) shows the distribution of the remaining oil saturation of binary flooding under edge water. The difference of the remaining oil saturation between strong edge water and no edge water is divided into positive and negative regions. The negative region is where the edge water action is beneficial to the remaining oil production, and the positive area is the unfavorable one (Figures 8(b) and 8(c)), respectively.

From Figure 8, the best area to exploit the remaining oil is confirmed to be between the edge water region and injection wells, while the effect of the edge water is clearly not conducive to produce the remaining oil in the area between injection and production wells. Hence, the presence of edge water is not beneficial to the overall production of the remaining oil, especially the remaining oil between the injection and production wells.

3.3. *Effect of Edge Water on Polymer Concentration.* With the increase in the polymer concentration, the solution viscosity increases. As a crucial factor in the polymer/surfactant binary flooding, the polymer viscosity can improve oil recovery via the control of the oil-water mobility. The change in concentration of the precursor polymer is the indirect reference to reflect the change in the polymer viscosity. By sampling and analysis, the variation diagrams of the polymer concentration fields with different injection volumes (0.3 PV and 0.6 PV; the following waterflooding is carried out until



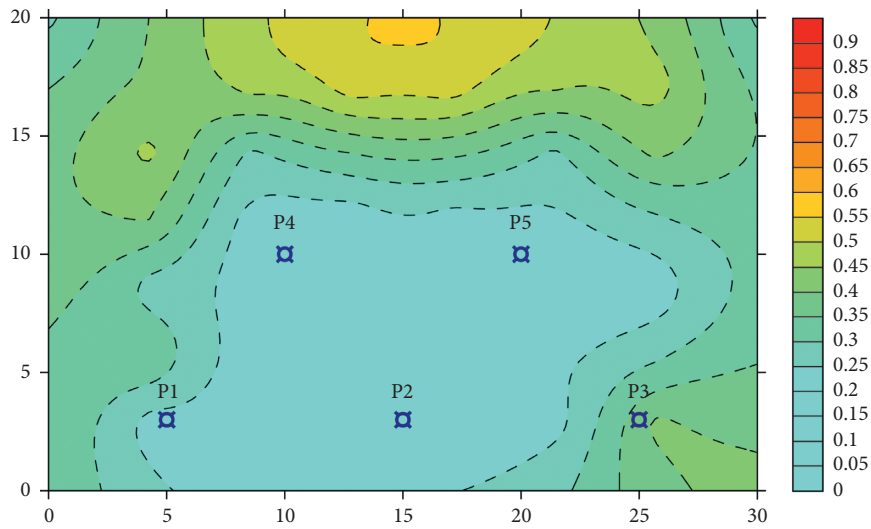


FIGURE 6: Remaining oil saturation distribution of binary flooding with no edge water.

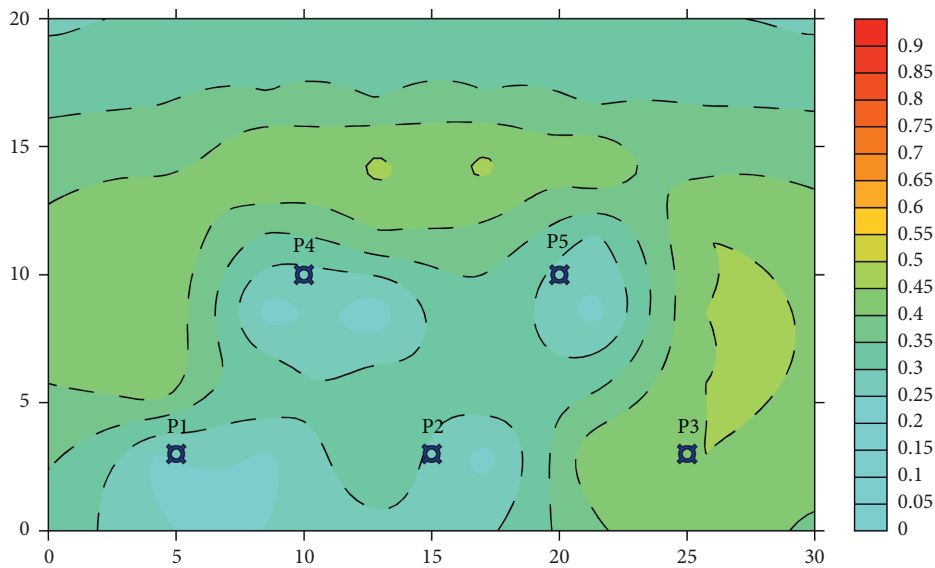


FIGURE 7: Remaining oil saturation distribution of binary flooding with strong edge water.

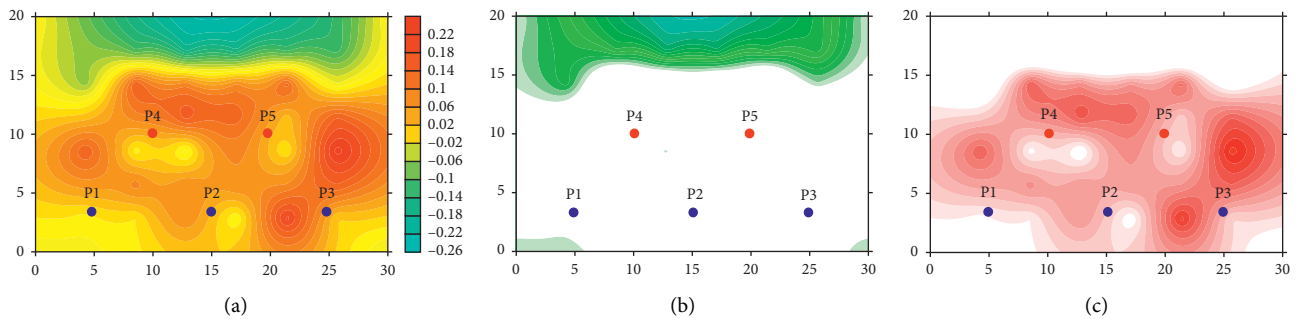


FIGURE 8: Difference diagram of the remaining oil saturation during binary flooding under different water energy conditions. (a) Whole region. (b) Negative region. (c) Positive region.

the water cut is 98%) in the chemical agent injection process with no edge water, weak, and strong edge water are obtained (Figures 9–11, respectively).

With the increase in the polymer injection volume, the polymer distribution region exhibits a “heart-shaped” expansion potential, and the concentration gradually increases

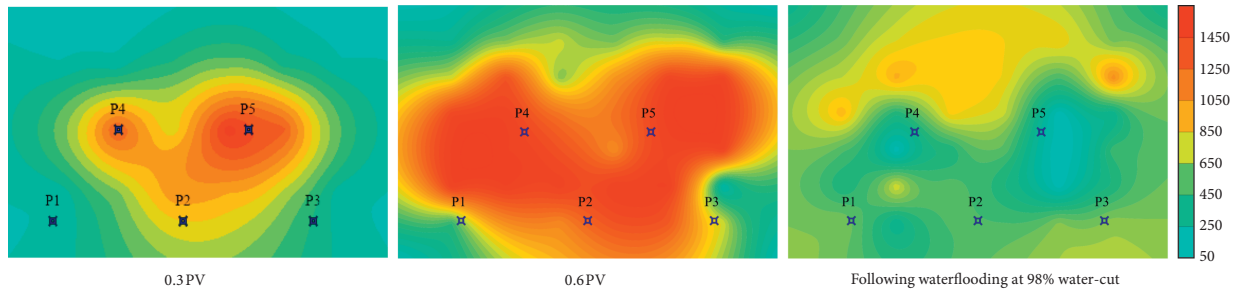


FIGURE 9: Variation of the polymer concentration field during chemical injection with no edge water.

under the no edge water condition (Figure 9). With the injection of 0.6 PV, the polymer is mainly distributed in the areas near injection well 1 and injection well 2 and between injection and production wells; the following water flooding process drives the polymer outside the “heart shape,” i.e., outside the injection-production wells; and the polymer concentration decreases accordingly.

When the same volume of the chemical agent is injected, the distribution area and concentration of the polymer under the three conditions of no edge water, weak edge water, and strong edge water, respectively, decrease in turn (Figures 10 and 11). Under the edge water condition, with the injection of 0.6 PV, the polymer mainly distributes between injection well 1, injection well 2, and production well 2. The range of the polymer distribution under the strong edge water condition is less than that under the weak edge water condition, that is, the “heart” area is smaller and the concentration is lower.

**3.4. Dilution Multiple.** To compare the concentration difference of the polymer flooding front under different edge water energy conditions, the dilution multiple concept is defined, which is the ratio of the chemical concentration with no edge water and with edge water; the dilution multiple characterizes the dilution degree of the edge water to the chemical agent.

The dilution multiple of the polymer concentration under strong and weak edge water conditions is converted into field diagrams (Figures 12 and 13). At the chemical injection stage, the invasion of edge water dilutes the polymer concentration. The stronger the edge water energy, the higher the dilution multiple. The area percentage of the strong edge water dilution to the chemical agent is 83% and that of the weak edge water dilution to the chemical agent is 48%.

The dilution degree is different in different areas, and the dilution area is mainly distributed in the area between the injection well and edge water (Figures 12 and 13). The dilution multiples of different regions are quantitatively evaluated by taking the average value (Figure 14). The dilution multiple between the injection well and edge water in a strong edge water reservoir is 2.2, while that between injection wells and production wells is only 1.3. In the weak edge water reservoir, the dilution multiple between the injection well and edge water is 1.6, and the dilution multiple between injection wells and production wells is 1.1. The

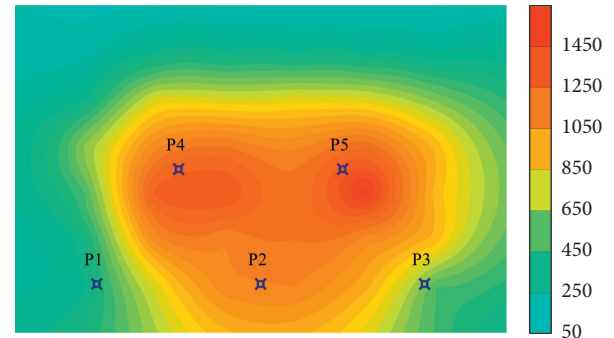


FIGURE 10: Polymer concentration field during binary flooding with weak edge water (0.6 PV).

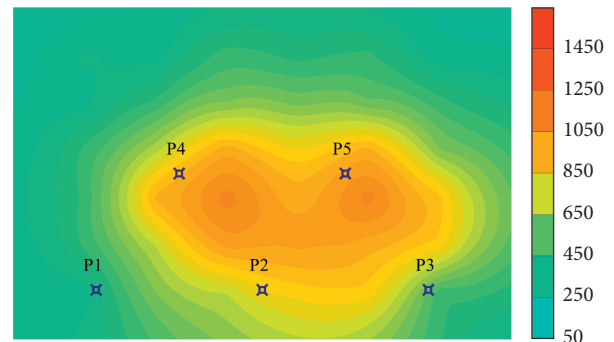


FIGURE 11: Polymer concentration field during binary flooding with strong edge water (0.6 PV).

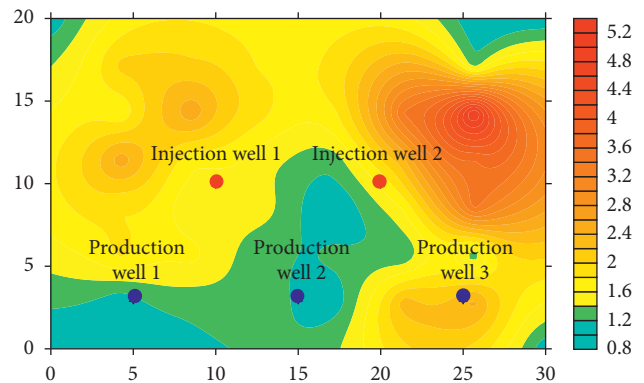


FIGURE 12: Field diagram of the dilution multiple after the chemical agent injection of 0.6 PV with strong edge water.

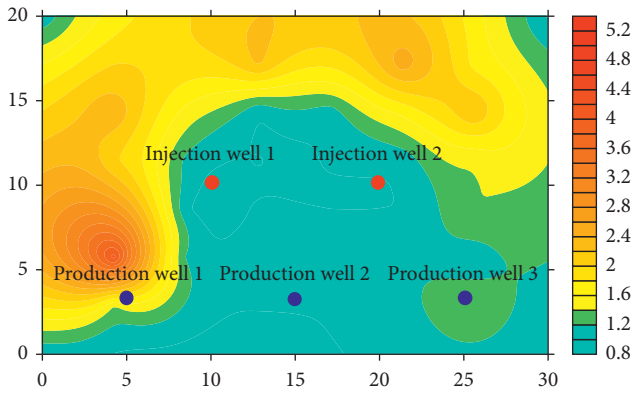


FIGURE 13: Field diagram of the dilution multiple after the chemical agent injection of 0.6 PV with weak edge water.

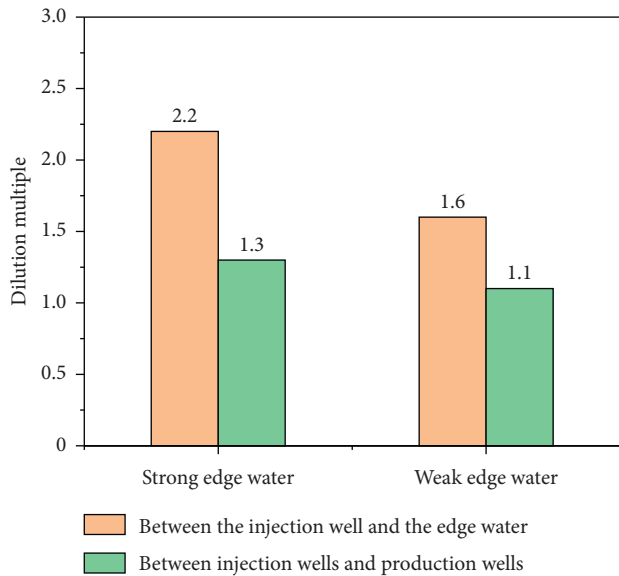


FIGURE 14: Dilution multiple of different regions under the strong and weak edge water conditions.

dilution multiple between the injection well and edge water is greater than that between the injection wells and production wells.

The dilution multiple and development effect of the polymer/surfactant binary flooding under different volumes of water invasion and different edge water energy conditions is compared (Figures 15 and 16). The invasion multiple of edge water considerably affects the dilution degree of the polymer. With the increase in the edge water invasion, the dilution multiple of the polymer gradually increases and the recovery degree for chemical flooding slowly increases. With the increase in the water invasion volume from 0.05 PV to 0.4 PV, the polymer dilution multiple increases from 1.08 to 1.72 in the strong edge water reservoir, and the polymer dilution multiple increases from 1.05 to 1.36 in the weak edge water reservoir. The dilution degree of strong edge water is more obvious. The dilution of the edge water to the polymer leads to the decrease in the effective polymer concentration. The oil recovery loss rates for the binary

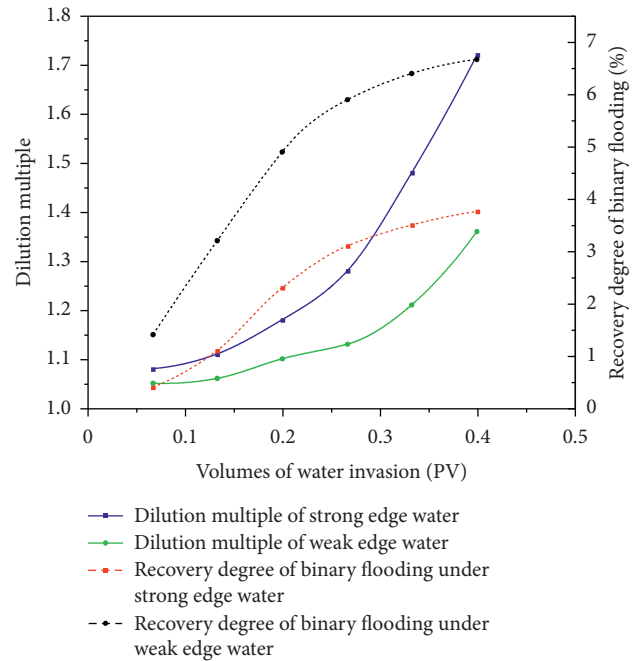


FIGURE 15: Dilution multiple under different volumes of water invasion and different edge water conditions.

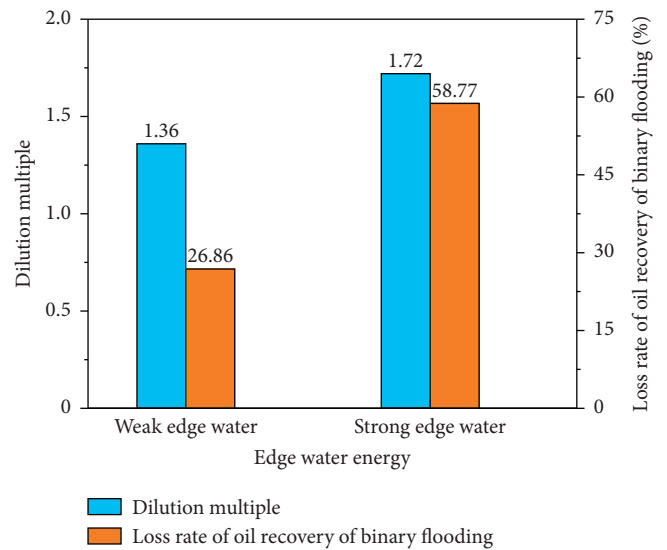


FIGURE 16: Effect of the edge water energy on the development effect of polymer/surfactant binary flooding.

flooding in the strong edge and weak edge water reservoirs are 58.77% and 26.86%, respectively. The stronger the edge water energy, the higher the recovery loss rate for the binary flooding.

#### 4. Practical Guidance

The dilution multiple reflects the dilution degree of the edge water to the chemical agent. In a majority of the reservoir areas, the chemical agent concentration is diluted by edge water, especially in the region between the injection well and edge water. The improvement of the well pattern of chemical

flooding near the water/oil contact and the maintenance of a reasonable injection-production ratio and injection rate are effective methods to control the invasion of edge water and improve chemical flooding EOR.

By taking the Ng8 reservoir of the Gao104-5 fault block in the North Gaoqian area of the Jidong Oilfield as an example, it is seen that the reservoir is a typical layered structural reservoir with edge water. After several years of development, the recovery degree and composite water cut are 28.3% and 96.0%, respectively. From the quantitative evaluation of the remaining oil, the residual remaining oil accounts for 66%, and the retained remaining oil accounts for 34%, which is mainly enriched in the top region among wells and the bypass areas along the water flooded path. The EOR technology should be adopted to improve the displacement efficiency. According to different occurrence states of the remaining oil, the differential design and combination of various displacement methods are carried out: binary flooding is implemented at the waist to improve the sweep efficiency and displacement efficiency; profile control is applied at the edge of the reservoir to plug the high capacity channel and adjust the invasion direction and invasion rate of edge water; and CO<sub>2</sub> huff and puff is carried out in the area beyond the well pattern control. Currently, the program is being implemented, and oil recovery is predicted to be improved by 10.22%.

## 5. Conclusion

- (1) Experimental results revealed that the recovery degree for binary flooding without edge water is the highest, and the one with strong edge water is the lowest. The reduction of the watercut during binary flooding without the edge water is the highest, while there is marginal difference between the weak edge water and strong edge water. The stronger the edge water energy, the worse the effect of binary flooding.
- (2) The concentration and distribution range of the chemical agent under the no edge water condition is clearly greater than that under the edge water condition, indicating that the chemical agent concentration can be "diluted" by edge water. The dilution degree is different in different areas, and the dilution is mainly located in the area between the injection wells and edge water.
- (3) With the increase in the invasion volume of edge water, the dilution ratio of the chemical agent gradually increases. The dilution of edge water to the chemical agent leads to the decrease in the effective chemical concentration. The stronger the edge water energy, the higher the dilution multiple, and the greater the recovery loss rate by binary flooding.

## Data Availability

The data used to support the findings of this study are included within the article.

## Conflicts of Interest

The authors declare that they have no conflicts of interest.

## Acknowledgments

This work was supported by the PetroChina Jidong Oilfield Company for research on special engineering of EOR (Project no. KF2018A03-01).

## References

- [1] B. Deng and W. Liu, "Water control of horizontal wells using foam-gel: lessons learnt in a heavy oil reservoir with strong waterdrive," in *Proceedings of the 2017 SPE/IATMI Asia Pacific Oil & Gas Conference and Exhibition*, Jakarta, Indonesia, October 2017.
- [2] J. Siemek and J. Stopa, "A simplified semi-analytical model for water-coning control in oil wells with dual completions system," *Journal of Energy Resources Technology*, vol. 124, no. 4, pp. 246–252, 2002.
- [3] E. M. Perez, F. Rodriguez De La Garza, and F. Samaniego-Verduzco, "Water coning in naturally fractured carbonate heavy oil reservoir—a simulation study," in *Proceedings of the 2012 SPE Latin America and Caribbean Petroleum Engineering Conference*, Mexico City, Mexico, April 2012.
- [4] X. Tu, D. L. Peng, and Z. Chen, "Research and field application of water coning control with production balanced method in bottom-water reservoir," in *Proceedings of the 2007 SPE Middle East Oil and Gas Show and Conference*, Manama, Bahrain, March 2007.
- [5] E. Shirif, "Mobility control by polymers under bottom-water conditions, experimental approach," in *Proceedings of the 2000 SPE Asia Pacific Oil and Gas Conference and Exhibition*, Brisbane, Australia, October 2000.
- [6] Q. Sun, Z. Li, S. Li, L. Jiang, J. Wang, and P. Wang, "Utilization of surfactant-stabilized foam for enhanced oil recovery by adding nanoparticles," *Energy & Fuels*, vol. 28, no. 4, pp. 2384–2394, 2014.
- [7] S. Bagci, "Seven-spot steam injection experiments in heavy oil reservoirs having a bottom water zone," *Energy & Fuels*, vol. 19, no. 3, pp. 1037–1046, 2005.
- [8] Z. Li, Z. Xu, B. Li et al., "Advances in research and application of foam flooding technology," *Journal of China University of Petroleum (Edition of Natural Science)*, vol. 43, no. 5, pp. 118–127, 2019.
- [9] B. Bai, J. Zhou, and M. Yin, "A comprehensive review of polyacrylamide polymer gels for conformance control," *Petroleum Exploration and Development*, vol. 42, no. 4, pp. 525–532, 2015.
- [10] Z. Li, C. Lin, Q. Shi et al., "Types of edge-water fault block reservoirs and features of residual oil in the Gaoqiannan area," *Journal of Southwest Petroleum University: Science & Technology Edition*, vol. 34, no. 1, pp. 115–120, 2012.
- [11] L. C. Li, S. L. Yang, and H. Chen, "Water and sand control technology successfully applied in Jidong oilfield: a case study," *Energy Sources, Part A: Recovery, Utilization, and Environmental Effects*, vol. 35, no. 24, pp. 2294–2301, 2013.
- [12] H. Li, D. Liu, J. Cui et al., "Remaining oil distribution regularity study of complex small fault block reservoir in extra-high water-cut period in south Gaoqian area," *Petroleum Geology and Engineering*, vol. 28, no. 4, pp. 74–156, 2014.

- [13] G. Zhang, "Analysis on IOR mechanism of artificial edge water flooding in complex fault-block reservoir," *Fault—Block Oil & Gas Field*, vol. 21, no. 4, pp. 476–479, 2014.
- [14] K. Xiao, H.-q. Jiang, and J.-j. Li, "Mechanisms of improving oil recovery efficiency by horizontal well in high water-cut stage," *Journal of China University of Petroleum (Edition of Natural Science)*, vol. 37, no. 3, pp. 110–114, 2013.
- [15] D. Han, "An approach to deep development of high water-cut oil fields to improve oil recovery ped," *Petroleum Exploration and Development*, vol. 22, no. 5, pp. 47–55, 1995.
- [16] Z. Xu, Z. Li, A. Jing, F. Meng, F. Dang, and T. Lu, "Synthesis of magnetic graphene oxide (MGO) and auxiliary microwaves to enhance oil recovery," *Energy & Fuels*, vol. 33, no. 10, pp. 9585–9595, 2019.
- [17] F. Zhao, "Research progress of chemical flooding enhanced oil recovery technologies in Shengli oilfield," *Petroleum & Petrochemical Today*, vol. 24, no. 10, pp. 19–22, 2016.
- [18] C. Zhou, Y. Xiao, and B. Zhang, "Progress of research work on chemical flooding technology in China," *China Surfactant Detergent & Cosmetics*, vol. 41, no. 2, pp. 131–135, 2011.
- [19] H. Pei, G. Zhang, J. Ge et al., "Advance in enhanced ordinary heavy oil recovery by chemical flooding," *Oilfield Chemistry*, vol. 27, no. 3, pp. 350–356, 2010.
- [20] X. Jia, G. Lei, and Z. Sun, "Review of horizontal well productivity water breakthrough in edge-aquifer oil reservoir with different drainage patterns," *Special Oil & Gas Reservoirs*, vol. 25, no. 5, pp. 1–7, 2018.
- [21] J. Zhao, D. Weng, P. Chen et al., "Experimental study on heterogeneous profile control physical simulation in edge water reservoir," *Advances in Fine Petrochemicals*, vol. 19, no. 1, pp. 32–34, 2018.
- [22] L. Wang, "Control measures of the boundary water in natural water drive reservoir," *Chemical Engineering Design Communications*, vol. 44, no. 1, p. 176, 2018.
- [23] J. Yin, C. Sun, D. Zhang et al., "The reasonable mining strength of high permeability and strong water reservoir," *Petrochemical Industry Application*, vol. 37, no. 1, pp. 70–73, 2018.